GSA Data Repository 2018024

Kent and Cooper, 2018, How well do zircons record the thermal evolution of magmatic systems?: Geology, https://doi.org/10.1130/G39690.1.

Supplemental Text

Modelling methodology

We have coupled several different aspects of zircon crystallization behavior in order to forward model zircon formation. The model, dubbed here "The Zirconator" is implemented in Visual Basic, running within Microsoft Excel and is freely available as a supplement to this paper and direct from the authors.

Firstly, we define the zircon saturation temperature and solidus for a given magmatic composition. For the examples shown in the paper we use a silicic endmember magma composition from Mount Hood with a zircon composition of 300 µg/g (Kent et al., 2010). Using R-MELTS (Gualda et al., 2012) we track the down temperature evolution of this magma in increments of 10°C from the projected liquidus at 930°C (at 200 MPa, with 4 wt.% H_2O). For each down temperature step, we calculate the zircon saturation temperature of the residual liquid using the formulation of Watson and Harrison (1983) and Boehnke et al. (2013) until the zircon saturation temperature equals or exceeds the magma temperature. For this composition zircon saturation occurs at 840°C using Watson and Harrison (1983) and 790°C using Boehnke et al. (2013). We use a zircon saturation temperature of 840°C for our modeling herein. The solidus is more difficult to define precisely using R-MELTS (Gualda et al., 2012), but we place it at 690°C.

We use the work of Harrison et al. (2007) to define the relative probability of zircon forming at a given temperature between zircon saturation and solidus. Harrison et al. (2007) modelled zircon crystallization for a representative intermediate granite composition and defined a monotonic decreasing curve of relative zircon crystallization rate between the saturation and solidus (Supplemental Figure DR1). Given that the relative rates of zircon formation at a given time also correspond to the probability of that age zircon being produced and then subsequently sampled, we use this curve to define the probability of zircon crystallizing at a given temperature (Supplemental Figure 1). To allow users to use this curve with different zircon saturation temperatures we define a monotonic decreasing curve between saturation and solidus temperatures following equation (1).

$$P = \left(1 - \left(\frac{T - T_{Sol}}{T_{Sat} - T_{Sol}}\right)^{a}\right)^{1/a} \qquad (1)$$

Where P is the probability between 0-1 and T_{Sat}, T_{Sol} are the temperatures of zircon saturation and the solidus. A value of a = 1.3 produces a curvature that matches that of Harrison et al. (2007).

We can likewise track dissolution, although the kinetics of zircon dissolution are less well understood. For temperatures 10, 20 and 30°C above zircon saturation we take the probability of dissolution or growth equal to 0, 0.33 and 0.66, and for higher temperatures the probability of dissolution is equal to one (Supplemental Figure DR1).

For this paper, we consider ages between 0 – 350 ka relevant to the U-Th system, although our approach is readily adaptable to zircon populations studied by U-Pb ages as well. We also largely limit ourselves to ages < 200 ka as uncertainties get larger as the U-Th systematics approach

secular equilibrium (e.g. Lowenstern et al., 2000). We track a large number (typically 10,000) synthetic “zircons” (representing potential zircons that can crystallize or dissolve) over 350 thousand years, in increments of 1000 years and 10°C. At each time step, we use the corresponding temperature from the user-defined thermal history to determine the relative probability of zircon growth and dissolution. For each “zircon” we compare a randomly generated number between 0-1 to the probability of zircon growth or dissolution consistent with the temperature. If the random number is less than the determined probability we consider growth or dissolution to have occurred. Where dissolution has occurred, zircon is removed (according to the ratio of growth and dissolution rates selected) from the youngest available zircon. For each potential “zircon” we track growth in one dimension and if no zircon remains no further dissolution occurs. Once we have completed these runs we compile the array of ages recorded and preserved in each of the synthetic zircons and the temperature at which each stage of zircon growth occurred to produce a distribution of zircon ages and temperatures.

The final part of our model takes into account the fact that: (i) analytical protocols sample only a small subset of the full array of zircon present in a given sample; and (ii) that additional dispersion of centroid values of age and temperature occurs due to analytical uncertainties. We simulate sampling using bootstrap techniques to randomly select (with replacement) members of the synthetic zircon population. The number of zircons selected in this process can be adjusted to reflect the numbers included in a typical analytical sample – in most studies this ranges between 10-50 individual analyses. To parameterize uncertainties in U-Th ages, we compared zircon age and uncertainty, using data from Barboni et al. (2016) and Klemetti and Clynne (2014) for U-Th ages for zircons. We fit a second order polynomial to this data to produce an empirical relation between age and uncertainty (Supplemental Figure DR2). Although uncertainties for U-Th ages

are somewhat asymmetric we simplify this by using symmetric errors. Uncertainties for Ti in zircon temperatures are taken as 20°C (1s) (Barboni et al., 2016). Although there are also potential inaccuracies for calculated temperature related to the activity of Ti and Si in coexisting melt, for this study we accept Ti in zircon temperatures as accurate.

To recreate the effects of analysis and uncertainty, bootstrap resampled zircons were randomly varied within the Gaussian distribution defined by 1s uncertainties in age and temperature. To do this we generated a random number between 0-1 for each sample and then used the percentage points of the normal distribution to equate each random number to a z-score, and used this to calculate the new centroid value. We ignored the small proportion of values predicted (~1%) to be outside ± 3s to avoid generation of extreme values for age and temperature. This approach produced values for age and temperature that are with ±3s of the true age and temperature, with a greater chance of values lying closer to the original centroid values in accordance with a Gaussian distribution.

Dissolution

When dissolution of zircon is indicated (by a temperature above zircon saturation), the model removes the youngest material available for each zircon we track, at a rate controlled by the dissolution rates input by the user. From this it is possible to model the effects of zircon dissolution of age-temperature systematics, however for this study we have also avoided thermal conditions that would cause dissolution (> 850°C for the composition we used). This is primarily because there are additional practical difficulties to understanding the potential role of

dissolution and to producing realistic zircon populations that result from dissolution. These include knowledge of the absolute dissolution rates and the relative rates of growth and dissolution (Watson, 1996; Bindeman and Melnik, 2016; Zhang and Xu, 2016). Users can input the growth and dissolution rates that they prefer, however the relative difference between growth and dissolution are the most important, and preservation of zircon is very sensitive to this. We track zircon growth and dissolution in 1D and where zircon dissolution rates are greater than growth rates by more than about a factor of 2-4 even very limited thermal excursions above saturation result in limited or no preservation of older zircon. There are also questions as to whether dissolution would remove the youngest available zircon (as we have implemented), or would preferentially remove older zones within zircon crystals, as textural examination of natural zircons reveals in some cases. Overall, we emphasize that any dissolution will also act to make it even more difficult to interpret thermal histories uniquely by removing older zircon from a system – and thus making older thermal excursions even more difficult to resolve.

Visual Basic Code

The “Zirconator” code that implements our zircon crystallization and sampling model runs as a Microsoft visual basic application within a Microsoft Excel spreadsheet. The file is supplied as a digital archive with this paper. Instructions for using the code are also provided.

2018024_The_Zirconator.xls

Supplemental Figure Captions

Supplemental Figure DR1. Relative probability of zircon growth and dissolution used for modelling. Zircon saturation and solidus temperatures are those determined for the Mount Hood composition used for this study (Kent et al., 2010). Symbols show probability at 10°C increments using zircon saturation temperatures (840°C, 790°C) calculated from and Watson and Harrison (1983) and Boehnke et al. (2013), and a solidus of 690°C.

Supplemental Figure DR2. Age vs. 1s uncertainties for U-Th age data sets from Klemetti and Clynne (2014) and Barboni et al. (2016). +1s and -1s uncertainties are shown as per legend. Curve represents least squares second order polynomial best fit to all data.

Supplemental references

Barboni, M., Boehnke, P., Schmitt, A. K., Harrison, T. M., Shane, P., Bouvier, A.-S., & Baumgartner, L. (2016). Warm storage for arc magmas. *Proceedings of the National Academy of Sciences*, *113*(49), 13959–13964. https://doi.org/10.1073/pnas.1616129113

Boehnke, P., Watson, E.B., Trail, D., Harrison, T.M., & Schmitt, A.K. (2013) Zircon saturation re-revisited. *Chemical Geology* 351, 324-334. http://dx.doi.org/10.1016/j.chemgeo.2013.05.028

Klemetti, E. W., & Clynne, M. A. (2014). Localized rejuvenation of a crystal mush recorded in zircon temporal and compositional variation at the lassen volcanic center, Northern California. *PLoS ONE*, *9*(12), 1–22. https://doi.org/10.1371/journal.pone.0113157

Gualda, G.A., Ghiorso, M.S., Lemons, R.L. & Carley, T.L. (2012) Rhyolite-MELTS: a modified calibration of MELTS optimized for silica-rich, fluid-bearing magmatic systems. *Journal of Petrology*, 53, 875-890.

Harrison, T. M., Watson, E. B., & Aikman, A. B. (2007). Temperature spectra of zircon crystallization in plutonic rocks. *Geology*, *35*(7), 635–638. https://doi.org/10.1130/G23505A.1

Kent, A. J. R., Darr, C., Koleszar, A. M., Salisbury, M. J., & Cooper, K. M. (2010). Preferential eruption of andesitic magmas through recharge filtering. *Nature Geoscience*, *3*, 631–636. https://doi.org/10.1038/NGEO924

Lowenstern, J. B., Persing, H. M., Wooden, J. L., Lanphere, M., Donnelly-Nolan, J., & Grove, T. L. (2000). U-Th dating of single zircons from young granitoid xenoliths: New tools for

understanding volcanic processes. *Earth and Planetary Science Letters*, *183*(1–2), 291–302. https://doi.org/10.1016/S0012-821X(00)00273-9

Watson, E.B., & Harrison, T.M. (1983) Zircon saturation revisited: Temperature and composition effects in a variety of crustal magma types. *Earth and Planetary Science Letters*, 64, 295– 304, https://doi: 10.1016/0012-821X(83)90211-X.

Watson E.B. (1996) Dissolution, growth and survival of zircons during crustal fusion; kinetic principles, geological models and implications for isotopic inheritance. *Special Paper Geological Society of America*, 315, 43–56.

Zhang, Y., & Xu, Z (2016) Zircon saturation and Zr diffusion in rhyolitic melts, and zircon growth geospeedometer. *American Mineralogist*, 101, 1252-1267.

Fig. DR1

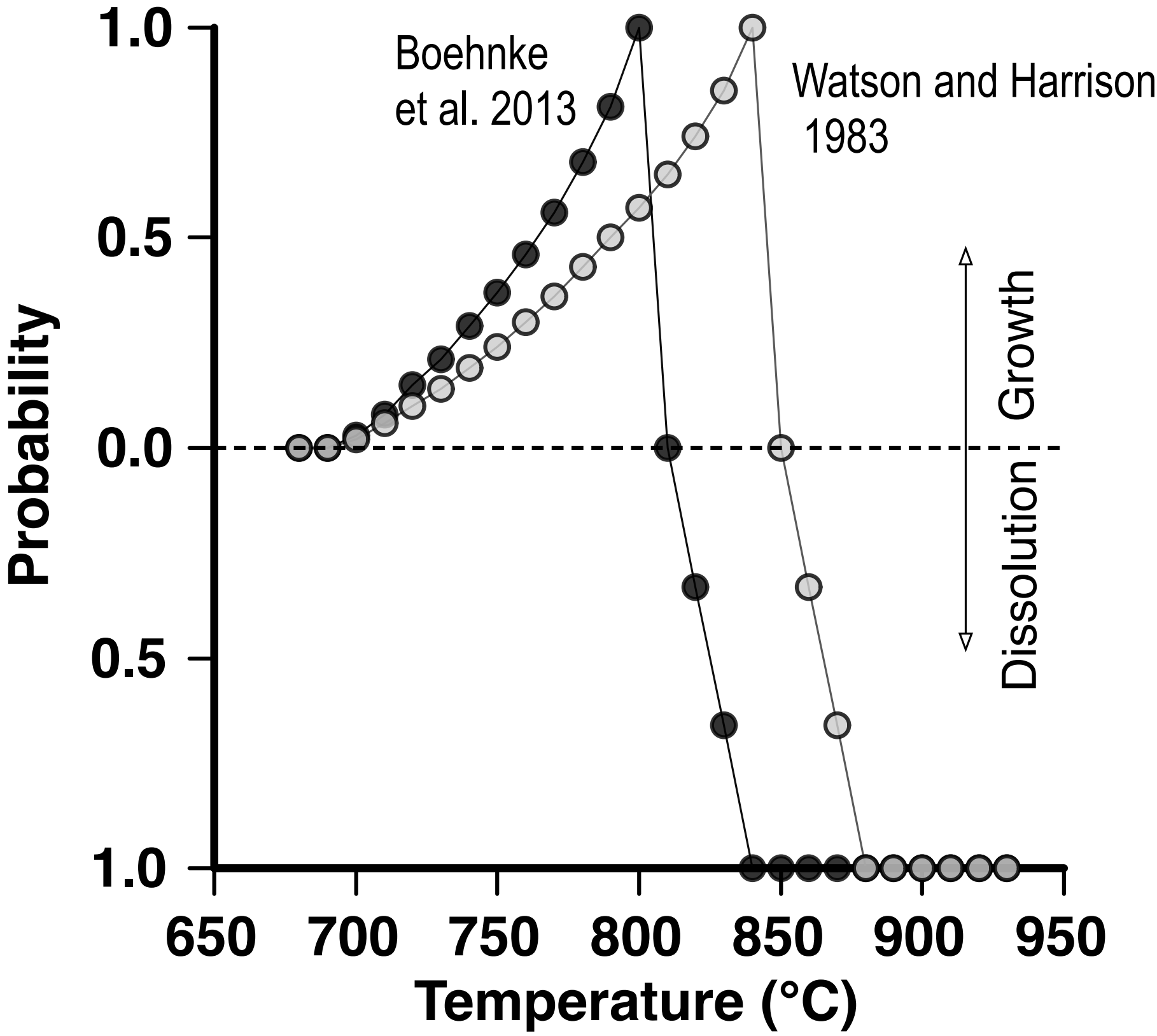
1.0
0.5
0.0
0.5
1.0
Probability
Boehnke
et al. 2013
Watson and Harrison
1983
Growth
Dissolution
650
700
750
800
850
900
950
Temperature (°C)

Fig. DR2

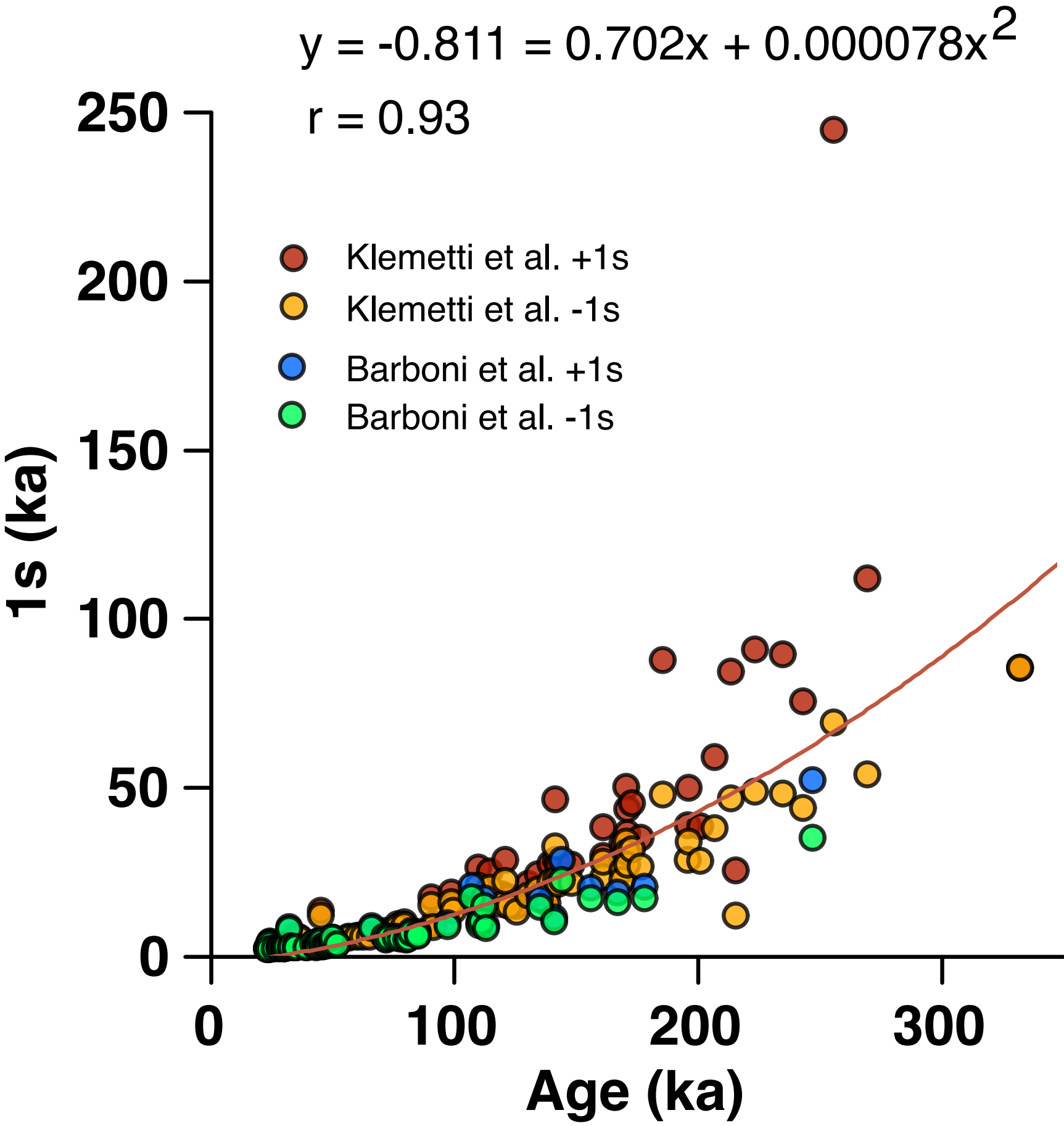
y = -0.811 = 0.702x + 0.000078x2
r = 0.93
Klemetti et al. +1s
Klemetti et al. -1s
Barboni et al. +1s
Barboni et al. -1s
1s (ka)
250
200
150
100
50
0
0
100
200
300
Age (ka)